OTC-29380-MS

Deposition Mitigation in Flowing Systems Using Coatings

Marshall A Pickarts, Center for Hydrate Research, Colorado School of Mines; Erika Brown, Oceanit Laboratories; Jose Delgado-Linares and Gabriela Blanchard, Center for Hydrate Research, Colorado School of Mines; Vinod Veedu, Oceanit Laboratories; Carolyn A Koh, Center for Hydrate Research, Colorado School of Mines

This paper was prepared for presentation at the Offshore Technology Conference held in Houston, Texas, USA, 6 – 9 May 2019.

Abstract

In pipelines, solid compounds including gas hydrates and asphaltenes may form/precipitate and accumulate on the pipe surface, leading to a gradual stenosis of the flowline. As a result, production may become increasingly difficult or possibly interrupted if mitigation efforts are not enacted. Typically, injected chemicals will either inhibit nucleation or dissolve already-formed deposits to restore original flow conditions back to the system; however, this can be a costly option. More recently, management strategies have been proposed where solids are handled in a controlled fashion rather than completely avoided. One such proposed management strategy as suggested for wall deposit formation is the use of coatings. Here, coatings can provide a low surface energy layer on the pipe wall, which restricts liquid and solid accumulation, allowing for a stable slurry flow through a system.

This study utilized two material formulations within several experimental setups to probe their interactions with water, gas hydrate, asphaltene, and crude oil. The results serve as part of an ongoing investigation into a surface treatment formulation that can be tested on larger-scale, fully flowing systems, which could be ultimately implemented into real-world production scenarios. The first surface treatment is a water-based polymeric surface that displays repellency to both oil and water phases (omniphobic). Testing of this material consisted of water contact angle measurements and static asphaltene/crude oil deposition quantification at atmospheric conditions, as well as visual confirmation of hydrate deposition prevention at high pressures. Additionally, an experimental superomniphobic surface treatment, which displays elevated resiliency to both water and hydrocarbons, was also examined within the asphaltene/crude oil test as a comparison to the omniphobic surface treatment.

Static contact angle results showed that the omniphobic surface treatment had reduced surface interaction with water droplets in air, increasing the low contact angles of corroded surfaces (0-31°) to slightly hydrophobic conditions of 91.5°. Additionally, rocking cells tests indicated that these omniphobic surface treatments may prevent gas hydrate deposition under high-pressure, semi-flowing conditions. Multiple tests found that formed hydrate agglomerants did not deposit for at least 48 and 72 hours. Finally, static deposition tests conducted in crude oil with forced asphaltene precipitation suggested that the omniphobic

surface treatment displayed a resistance to both asphaltenes and crude oil when compared to untreated and superomniphobic surfaces.

Introduction

Gas hydrates are nonstoichiometric crystalline solid compounds that comprise a subset of chemical substances known as clathrates, in which a host lattice structure traps guest molecules within cages (Sloan and Koh, 2007). In the case of gas (clathrate) hydrates, water molecules are hydrogen bonded together to form cavities that make up this host lattice structure. Suitably sized guest molecules, (<0.9 nm) such as methane, ethane, propane, or carbon dioxide may reside within these cages under the appropriate thermodynamic conditions (low temperatures and high pressures) (Sloan and Koh, 2007). Particularly in offshore oil and gas fields, conditions are favorable for gas hydrate formation, and production fluids often contain the materials necessary for hydrate formation (small guest molecules and water). As a result, the possibility of rapid hydrate formation and eventual accumulation into a plug can be significant, and hence requires mitigation control from operators (Koh et al., 2011).

The conventional method to address these hydrate concerns employ a complete hydrate avoidance strategy, where the injection of thermodynamic inhibitors (THIs), such as methanol or monoethylene glycol, shift the hydrate stable zone to harsher conditions (lower temperatures and higher pressures) (Sloan and Koh, 2007). However, issues associated with operational expenditures, flow properties, toxicity, and product contamination have limited THI application, especially in aging and deepwater fields (Patel, Zubin and Russum, 2010; Sloan et al., 2011). Consequently, newer "hydrate management" techniques have been proposed for cases where thermodynamic inhibitor use is inappropriate (Creek et al., 2011; Sloan, 2005). To enact this strategy, external chemicals known as low dosage hydrate inhibitors (LDHI) can be applied and/or combined with advantageous system properties (e.g. non-agglomerating oils, limited free water, etc.) and predictive knowledge from advanced analytics (numerical multiphase flow simulators) to enable safe and controlled operation within the hydrate domain (Creek et al., 2011; Kinnari et al., 2015).

To practice such a risk-based strategy requires a detailed understanding of hydrate formation/accumulation mechanisms and methods for their prevention/mitigation. Over the years, numerous studies have investigated various hydrate growth and particle interaction processes that may ultimately lead to jamming in a flowline (Aman et al., 2016; Creek et al., 2011; Ding et al., 2017; Lachance et al., 2012; Nicholas et al., 2009; Srivastava et al., 2017; Turner et al., 2005), as shown in Figure 1. These include hydrate bulk formation (shell growth on emulsified droplets), bedding (agglomerate settling), deposition (impingement with subsequent adherence of hydrate particle to pipe wall), and film growth (direct conversion of water to hydrate on pipe surface).

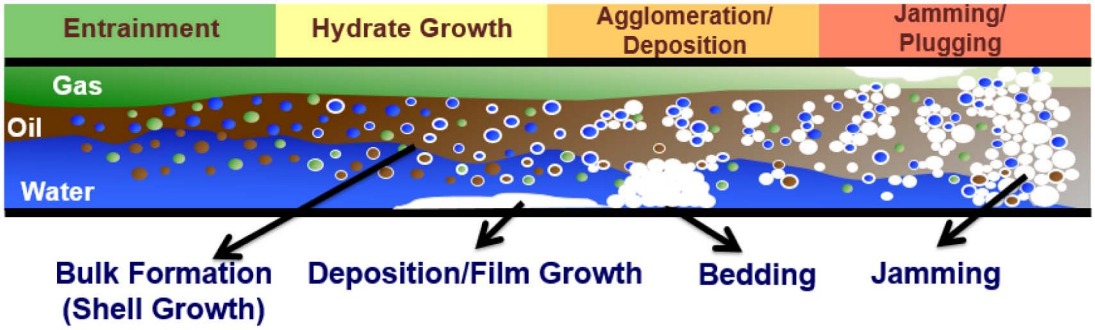

Figure 1—Conceptual picture illustrating hydrate formation and accumulation processes occurring in a flowline. Adapted from (Turner et al., 2005).

Additionally, field mitigation strategies (e.g. chemical injection) have been developed to address some of these identified processes. Currently, hydrate formation/shell growth and consequent agglomeration

and bedding can be managed with kinetic hydrate inhibitors (KHIs) and anti-agglomerants (AAs), which operate by disrupting nucleation sites and the liquid capillary bridge between hydrate particles, respectively (Anklam et al., 2007; Dirdal, 2013). However, recent investigations have indicated there is an outstanding need to mitigate hydrate film growth or deposition. Examples of such cases can be found throughout the literature (Ding et al., 2017; Lachance et al., 2012; Urdahl et al., 1995). Therefore, methods to address hydrate accumulation on the pipe wall through film growth and deposition remain a major outstanding issue.

In a laboratory setting, hydrate deposition and film growth mechanisms of direct liquid contact, liquid capillarity, and water evaporation/condensation have been identified (Grasso et al., 2014), where each of these mechanisms has a common preceding step of water wetting on the pipe wall. The presence of this water wetting complements earlier observations made during micromechanical force experiments in which a water capillary bridge forms between a surface and an individual hydrate particle (shown schematically in Figure 2), resulting in the measured adhesive forces of these deposited particles (Aman et al., 2011; Wang et al., 2017). A coating study investigated adhesion and hydrophobicity, which was tuned through the surface energy and correlated by water contact angles, to a reduction in hydrate adhesion (which may possibly scale up to deposition in flowing systems) (Smith et al., 2012). Additional promising results have been reported for tetrahydrofuran and cyclopentane model hydrates on polymeric-fluorine rich bilayer, omniphobic, and superhydrophobic coatings (Brown et al., 2017; Sojoudi et al., 2018, 2015).

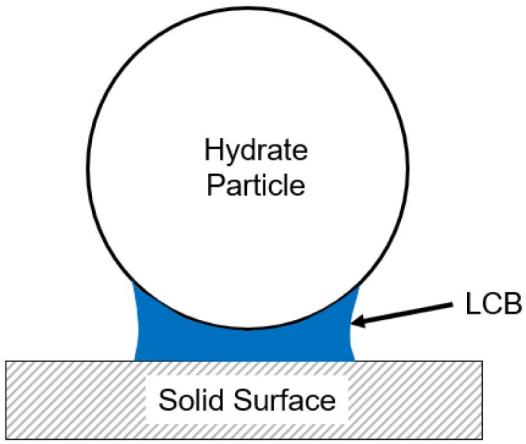

Figure 2—Liquid capillary bridge (LCB) formed between hydrate particle and solid surface. Redrawn from (Aman et al., 2011).

The buildup of solid particles on pipe walls is not unique to hydrates however. Reports show similar phenomena occurring in both waxes and asphaltenes (*i.e.*, the most polar fraction of crude oil that is insoluble in paraffins, but soluble in aromatics), where pipeline coatings/surface treatments have been proposed as a possible mitigation strategy over previously used dissolving solvents and chemical inhibitors (Ellison et al., 2000; Gharbi et al., 2017; Kelland, 2014; Kokal and Sayegh, 1995; Speight, 2004). Here, authors stress the importance of understanding deposition and adhesion mechanisms first, which then feed into the successful development of anti-wax and anti-asphaltene surfaces (Paso et al., 2009; Sousa et al., 2019; Vargas, F. M., Tavakkoli, 2018). One case using this methodology has already been presented, where a hydrophobic molecularly bonded coating showed encouraging results for scale, wax, and asphaltene deposition reduction in flowloop and field trials tests (Bethke et al., 2018).

While the potential for coatings as a general deposition mitigation strategy has been demonstrated, most of the previous studies have focused efforts as initial studies on a singular flow assurance issue (*i.e.*, wax, asphaltene, or hydrate) and/or model, low-pressure, small-scale, or static systems. Without the means to advance to more realistic scenarios (*i.e.*, large-scale, high-pressure, fully-flowing, and non-model setups), it can be difficult to identify a formulation that can be extrapolated to an industrial setting. The ultimate focus of this study lies in the development of a robust pipeline coating/surface treatment capable of reducing

deposition behavior of multiple solids, and that can be readily applied to existing large-scale industrial production systems. The work presented in this paper comprises part of an ongoing study to identify and develop potential surface treatment formulations that could be scaled-up for future testing on equipment such as a flowloop and meet the stated requirements above.

Methods and Materials

Materials

The primary material targeted in this study is a water-based polymeric surface treatment which displays omniphobic properties, demonstrating repellency to both water and oil phases. The omniphobic properties allow the material to be used in a variety of applications as it is not fouled by oil, as are many hydrophobic coatings. The omniphobic surface treatment used in this study was developed to prevent corrosion, or, when applied to a corroded surface, to restore properties such as repellency and surface roughness to better-than-new conditions. In Figure 3, comparisons are shown for treated and untreated coupons, showing that not only is the omniphobic treatment resistant to corrosion in extreme conditions, but that the surface retains its hydro- and oleophobicity.

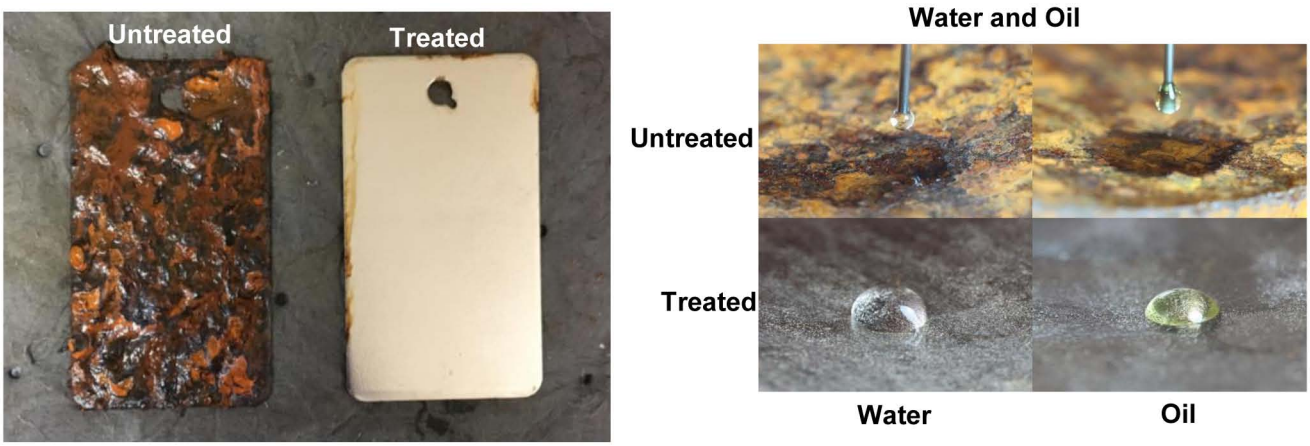

Figure 3—Results of salt fog corrosion testing for treated and untreated coupons. The omniphobic treatment is corrosion resistant and remains hydrophobic and oleophobic even after significant exposure.

The oleophobic treatment has been tested for its chemical compatibility and abrasion resistance. Due to the high degree of performance combined with the low surface energy and water repellant properties shown by this material, it was selected as a primary candidate for hydrate repellency. Previous studies using an earlier version of this material showed a reduction in hydrate adhesion force of 10x (Brown et al., 2017). However, because the material is also repellant to oil-based chemistries, it is also a candidate for a general flow-assurance promotor, potentially a candidate for resisting deposition from waxes and asphaltenes, in addition to hydrates.

The omniphobic treatment was tested for compatibility with a number of chemicals which may be common in oil and gas production lines, with a focus on hydrocarbons and aromatics, which are known to interfere with polymers. The fluids selected for testing were:

- Kerosene
- Xylene
- JP8

JP8, or Jet Propulsion Fuel 8, is a mixture of hydrocarbons as well as additives with several solvents that were of interest for testing. A general composition of JP8 is given in Table 1. The aromatic fraction of JP was especially of interest as it contains compounds such as benzenes and toluene.

Table 1—JP8 chemical composition

Compound	Approximate Amount
C8-C9 aliphatic hydrocarbons	9%
C10-C14 aliphatic hydrocarbons	65%
C15-C17 aliphatic hydrocarbons	7%
aromatics	18%

The treatment has been tested in the past for resistance to acids, bases, and oils. Coupons which were fully coated on both sides were submerged halfway into the test fluids and were inspected periodically for changes in appearance, weight (for swelling or dissolution), and adhesion. Images are shown in Figure 4. Coupons were tested for 120 days. For kerosene and JP8, no visual changes, mass changes, or apparent changes in adhesion were detectable even after four month's complete submersion. Xylene showed a slight lightening of the surface coloration, but there was no mass loss or gain and the adhesion appeared unaltered.

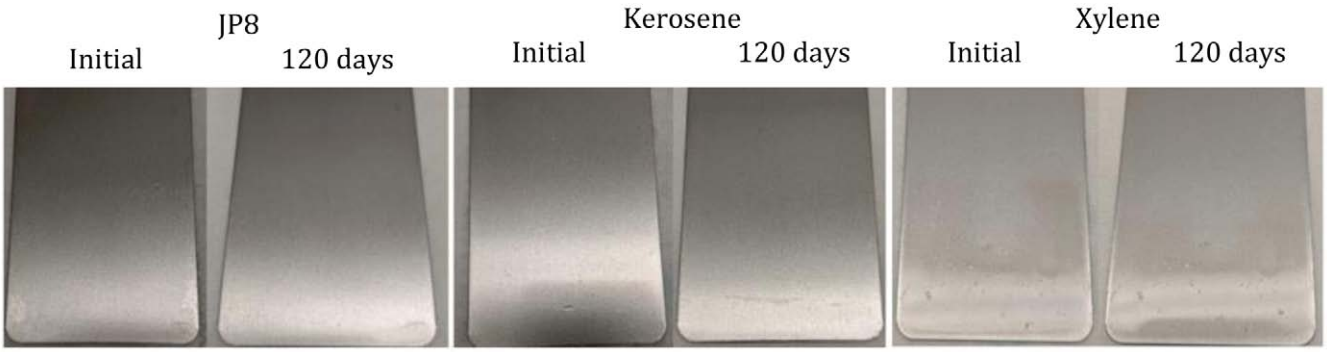

Figure 4—Treated and untreated coupons after 120 days submersion in test fluids.

Abrasion testing was also conducted using ASTM D4060 under the following conditions.

- Instrument – Rotary Abraser
- Abrasive Wheels – CS-17
- Vac. Nozzle Gap – 1/8"
- Total Cycles – 1000
- Test Load – 1000 g
- Test Conditions 74 F, 53% RH

It was found that the total mass lost averaged 50 mg, which compares favorably to epoxy in terms of expected lifetime under erosion conditions.

The second treatment used in this study is a new, experimental superomniphobic treatment, which is still in the developmental stages. This material has shown extreme repellency for both water and hydrocarbons (>120°). However, the abrasion resistance and adhesion to surfaces on this treatment have not yet been

optimized. The purpose of investigating this material is to determine the relative importance of surface energy and to test the new material for its viability at resisting deposition of different materials.

Interfacial Tensiometer (IFT)

When coupled with the appropriate software, the IFT is capable of measuring surface tension and/or contact angles of pendant (drop in liquid/gas phase) and sessile (drop on solid surface) droplets based on drop shape analysis. The apparatus consists of four major components for performing experiments: an optical camera, light source, cuvette, and syringe. The CCD camera faces a monochromatic LED based light source. A 40mm × 20mm cuvette and luer tip 1mL syringe lie between the camera and light source, providing the environment (static conditions, bulk phase) and materials (water, oil, etc.) necessary to perform experiments. Together, these components rest on a Vibraplane isolation plate to reduce vibrational interference.

To obtain the desired surface tension or contact angle values, the computer software linked to the experimental apparatus performs a series of image analysis techniques and calculations. This process starts when the computer gathers images captured by the CCD camera during the experiment to determine a droplet profile. Once found, the program extracts this droplet profile and fits it to the Young-Laplace equation (Equation 1), which then feeds into the calculation of the static contact angle (Equation 2). The calculation process concludes when the software uses the values determined from the fitting to compute either surface tension or contact angle.

$$\Delta P = \gamma_{lv}\left(\frac{1}{R_1}+\frac{1}{R_2}\right) \tag{1}$$

$$\cos\theta = \frac{\gamma_{sv}-\gamma_{sl}}{\gamma_{lv}} \tag{2}$$

In Equation 1, ΔP represents the pressure difference across the liquid interface. It is determined numerically using the difference between known densities of the fluids used in the experiment. γ_{lv} is the interfacial tension between droplet and bulk phase. R_1 and R_2 are the radii of curvatures of the droplet, taken at the same tangent position, but perpendicular to each other. Finally, θ, γ_{sv}, and γ_{sl} are the static contact angle and interfacial energies between solid surface-bulk phase and solid surface-droplet.

Before each new experiment, the apparatus is recalibrated to ensure that the camera is focused on the correct spatial position of the experiment (specific location on stage). This is done with a calibration ball of known size (4.000 mm). With the completion of the calibration test, the sessile drop experiments commence. Here, the cuvette is thoroughly cleaned to remove any fluids from the calibration/previous tests and filled with the desired light liquid phase (such as oil). A surface for the contact angle measurement is also placed inside the cuvette and submerged in the liquid phase. The syringe is filled with the desired heavy liquid phase and placed within the holder above the cuvette. A droplet is slowly dispensed from the syringe onto the measuring surface. A 20 second waiting period ensues to ensure the system has reached an equilibrium state for static contact angle measurements. At this point, contact angles are recorded each second in 10 second intervals, specifying the analysis mode as Young-Laplace.

High Pressure Rocking Cell

The rocking cell apparatus consists of three identical high-pressure visual cells, shown schematically in Figure 5. Each cell comprises of a custom stainless-steel body sealed with O-rings and two sapphire glass tubes for visualization. The bodies of all three cells are connected with a custom-built polytetrafluoroethylene rocking holder and rotated to 20° angles using a DC motor. The entire assembly is cooled inside an acrylic water bath using a chiller attached to a copper pipe cooling network. During experiments, cell pressures and the bath temperature are recorded.

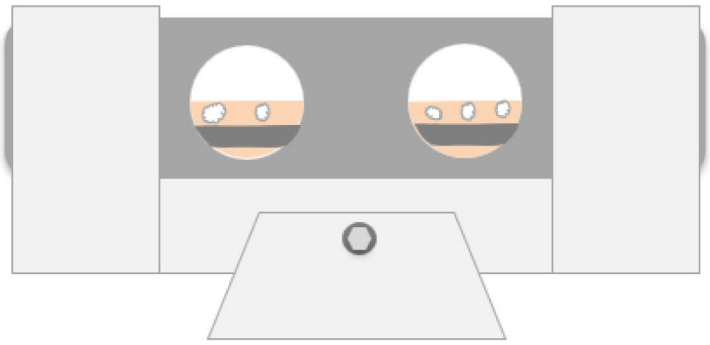

Figure 5—High pressure rocking cell setup consisting of stainless steel body, sapphire glass visualization windows, and PTFE rocking mechanism. Cell contents containing of model oil, DI water/hydrate, methane/ethane gas, and a treated/untreated carbon steel coupon.

Experiments start by loading the rocking cells with the desired liquids (model oil and DI water), so that the proper liquid holdup and water contents were provided. A stainless-steel coupon, which may be treated or untreated, was then placed at the bottom of each cell, and the cells were sealed shut with screw caps. The rocking cells were then slowly pressurized at ambient temperatures with 74.7/25.3 mol.% methane/ethane gas to 1000 psig. These conditions were maintained until gas saturation in the liquid phase reached an equilibrium. At this point, the DC motor rocked the cells to facilitate mixing of the system's contents for several hours.

The chiller was then programed to cool the rocking cells into the hydrate formation region over a period of 6 hours to a final bath temperature of 2.5°C. This temperature was held throughout the experiment as hydrates formed and the system reached an equilibrium state. Hydrate formation was detected through visual observation and a sudden drop in cell pressure, since these operated under a constant volume mode. Experiments concluded when hydrate formation ceased, typically due to complete consumption of hydrate forming materials, and the bath was returned to ambient temperature for hydrate dissociation. Results were analyzed through visual observations made during the experiments where treated/untreated coupons were assessed for their hydrate deposition prevention/mitigation ability.

Results and Discussion

Contact Angle Measurements

In this work, five different surface types were utilized. Results are presented for contact angles of DI water droplets on untreated/treated carbon steel surfaces in an ambient air bulk phase. Within each experimental condition, 5 droplets were analyzed on 3 separate coupons. Data points become an average of left and right contact angles for these 15 trials and the final contact angle for the surface type pairing is given as an average of all data points recorded.

Data collection began with untreated pristine carbon steel coupons in air, which served as a baseline for benchmarking with literature results. From these tests, it was found that untreated pristine carbon steel coupons were slightly hydrophilic with a contact angle of ~83°. This was consistent with previously reported contact angles on carbon steel AISI 1045 (Tsai et al., 2015; Zhang et al., 2015). Further contact angle measurements conducted on untreated corroded surfaces (what one would typically find in the field) found that wetting increased drastically, ranging from a 0° fully wet surface to 31°. However, when an omniphobic surface treatment was applied to a carbon steel coupon, the water contact angle could be increased to better-than-new values. This corresponded to a surface that was now slightly hydrophobic at 91.5°, representing a ~10% increase in the contact angle over a pristine untreated surface and a dramatic transformation from the corroded surfaces. The results from these experiments are displayed visually in Figure 6 and graphically in Figure 7.

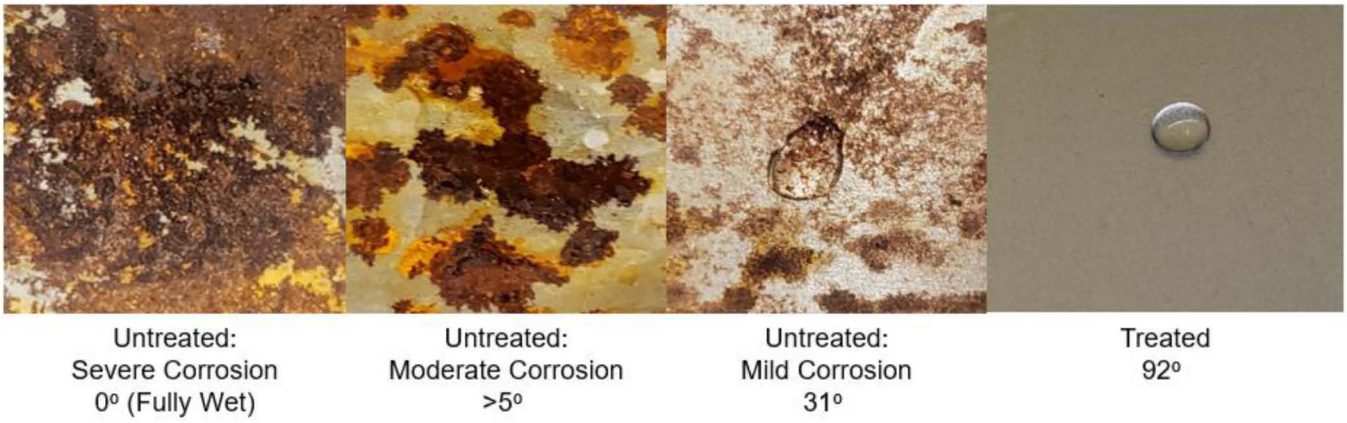

Figure 6—Water droplet wetting on various surfaces: untreated with severe corrosion, untreated with moderate corrosion, untreated with mild corrosion, and treated.

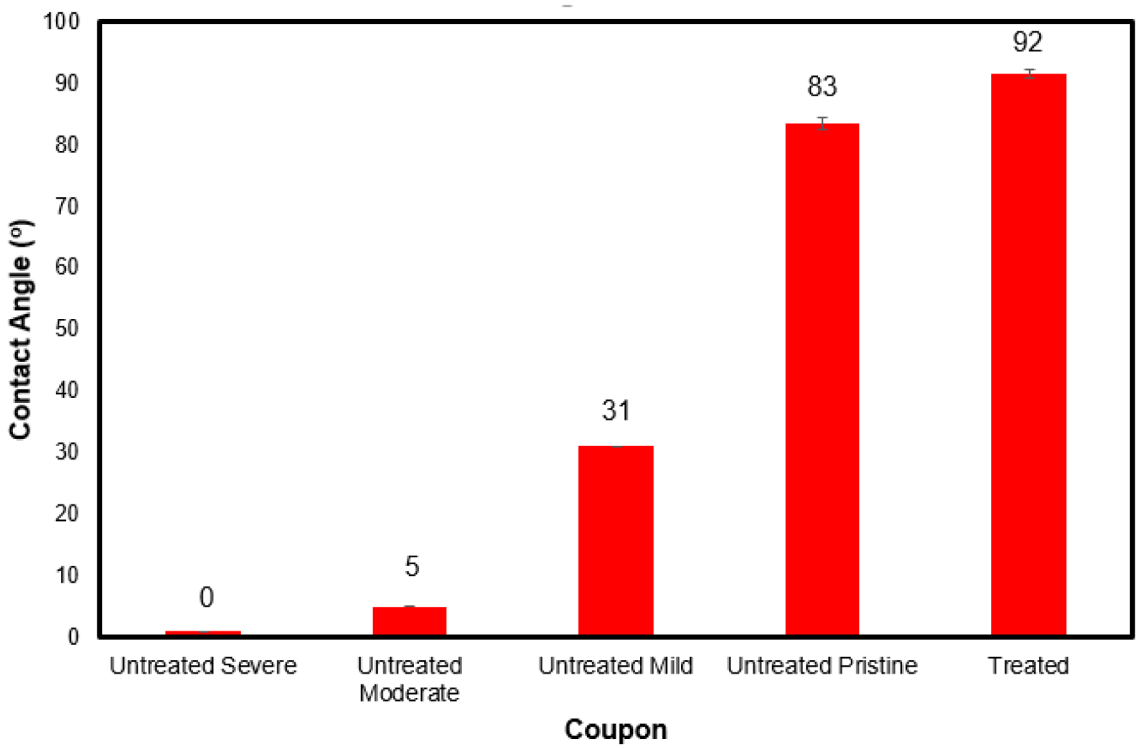

Figure 7—Static contact angle measurements for untreated/treated surfaces in air. Results show treated surfaces can restore surfaces to better-than-new conditions, increasing the low contact angles of corroded surfaces to slightly hydrophobic conditions. Error bars represent 95% confidence intervals in the results.

Rocking Cell Screening Tests

The next screening tool utilized in this study was the rocking cell system. Here, the omniphobic surface treatment's gas hydrate deposition resistance was evaluated at high pressure (1000 psig), shear-induced conditions in a similar fashion to Brown et al., 2017. In particular, this surface treatment was tested to identify whether it is a viable candidate for further experimentation in a lab-scale flowloop. These tests were conducted with model oil, DI water, and a 74.7/25.3 mol.% methane/ethane gas mixture at 50% liquid holdup and 5% watercut.

In the untreated coupon tests, hydrates formed quickly (*i.e.*, before coated samples) throughout the cell as thin depositing layers on the coupon edges and balled agglomerants on its faces (see Figure 8a). Treated coupons, on the other hand, tended to only form unadhered balled agglomerants that rolled across the cell.

Figure 8b shows an example of one such test where hydrates formed, but remained in the bulk liquid as a flowable slurry. This behavior was observed for at least 48 hours (when tests were concluded and hydrates dissociated). This result was repeatable with coupons displaying the ability to resist gas hydrate deposition until forced hydrate dissociation (between 24 and 72 hours).

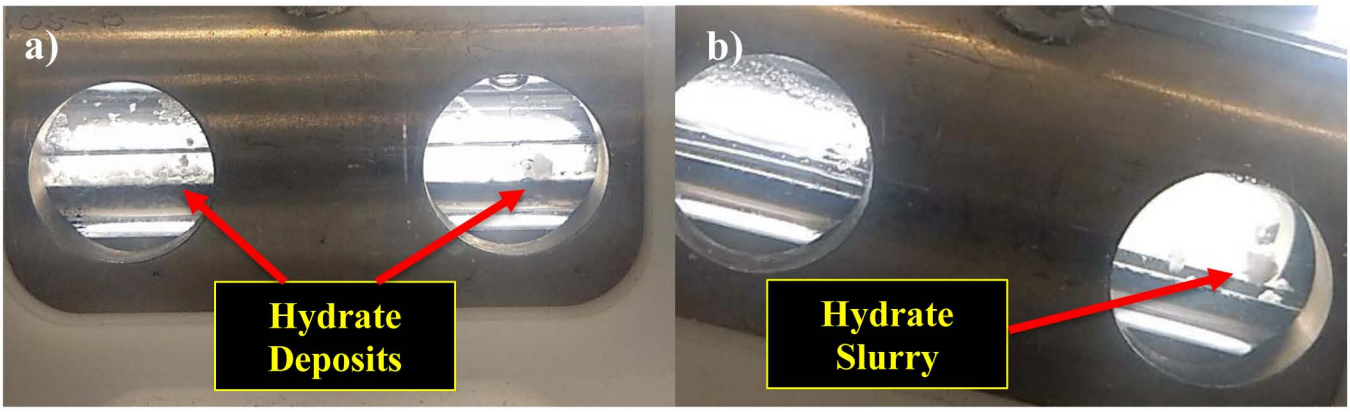

Figure 8—High pressure rocking cell tests at 50% liquid loading, 5% watercut. a) Multiple hydrate deposits adhered to untreated coupon surface. b) Flowable hydrate slurry observed on omniphobic treated coupon cell 48 hours after hydrate nucleation.

Asphaltene/Crude Oil Deposition Tests

In addition to hydrate deposition, the surface treatment's effect on asphaltene deposition was investigated. Asphaltenes were precipitated onto an untreated/treated coupon in a static system to observe and quantify the amount of deposited solids/liquid and estimate the initial resistance of the surface treatment to asphaltene deposition. By doing this, the system was simplified (initially without the presence of shear and other depositing solids, such as gas hydrates) for more controlled preliminary testing and analysis.

Coupons were weighed prior to the asphaltene precipitation experiments, then placed in a metal container with n-heptane (500 mL). To induce asphaltene precipitation, 10 vol% of crude oil (50 mL; this crude oil has a C_7-asphaltene content of 3.07 ± 0.23 wt.% and is stable in terms of asphaltene precipitation) was mixed with n-heptane, while agitating the solution with a magnetic stir bar. After 5 hours, the stirring was stopped and the mixture (coupon + n-heptane + crude oil) was left to settle overnight. The coupon was then removed from the solution, gently agitated to remove the non-adhered solid, held vertically for 10 seconds, and placed into the oven for 24 hours at 50 °C. Finally, the dried coupon was weighed to determine the amount of asphaltenes/residual liquids deposited on the surface. This test was performed for three coupons, an untreated and two treated (superomniphobic and omniphobic), and repeated three times for each coupon.

Figure 9 presents the average and the standard deviation of the ratio of *mass of deposited material / mass of coupon*. The trends for these initial tests are consistent with the visual images in Figure 10, where the omniphobic surface treatment was the least likely to accumulate asphaltenes. This is in contrast to the untreated coupon in which the highest accumulation of asphaltenes was observed. The large error bars seen for each surface are the result of significant differences in overall deposition within each trial. However, the general trend seen in Figure 9 is observed within each trial set.

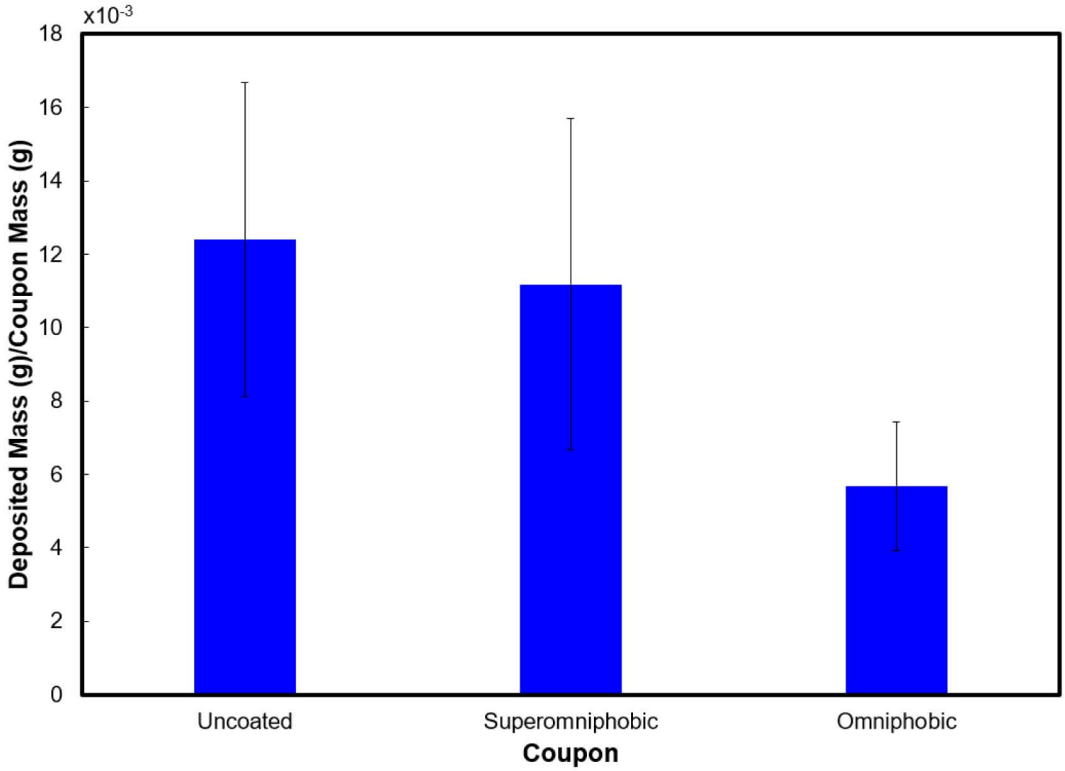

Figure 9—Average of the mass of the deposited material/mass of coupon ratio versus kind of coupon tested (3 repeat tests). Preliminary analysis indicates that ~35% of this deposited mass is comprised of asphaltene deposits.

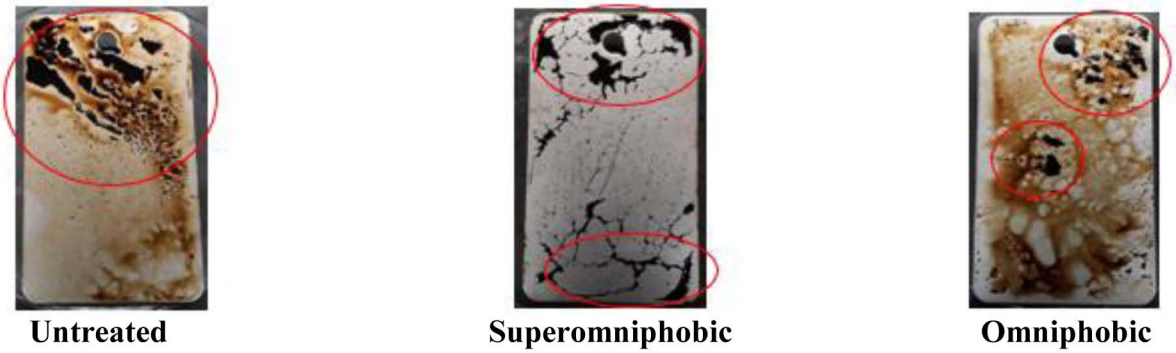

Figure 10—Images of coupons after asphaltene deposition in static precipitation tests (asphaltene deposits are marked with a red circle/oval).

Conclusions

Compared to agglomeration (particularly with hydrates), solid deposition and hydrate film growth processes remain major outstanding flow assurance issues. The ability to prevent or even mitigate the stenosis of pipe walls would be a remarkable achievement for management strategies. Pipeline coatings with the ability to preclude solid/liquid accumulation on their surfaces have shown promise in this area. In this study, a class of omniphobic surface treatments demonstrated the ability to reduce water, hydrate, asphaltene, and crude oil accumulation on their surfaces. Under static, atmospheric conditions, these omniphobic surface treatments increased water droplet contact angles to better-than-new conditions (from 0° fully wet in severely corroded systems to 91.5°) in an air bulk phase. Furthermore, when taken to high pressure, these surface treatments repeatedly displayed the ability to avoid hydrate deposit formation for several days. Finally, when initially tested in a crude oil system, the omniphobic surface treatment exhibited the ability to decrease asphaltene and crude oil deposition on its surface when compared to untreated and superomniphobic surfaces. These

results present promising first steps in an ongoing solids deposition prevention investigation for surface treatment formulations that display desired repellency properties. Subsequent efforts will focus on further development and scaling of the selected formulations up to high pressure flowloop testing so that a robust, appropriately tested surface treatment can be ultimately be recommended for application to industrial settings as part of solids management strategies.

Acknowledgement

The authors would like to acknowledge the support from the U.S. DOE-NETL for funding this work, and William Fincham, DOE-NETL Program Manager for support and advise on this work. Special thanks to Davi Salmin and Siija Hu for their guidance and support during experimental setup. Additional thanks to Yan Wang for her proofreading and valuable comments related to this work.

References

Aman, Z.M., Brown, E.P., Sloan, E.D., Sum, A.K., Koh, C.A., 2011. Interfacial mechanisms governing cyclopentane clathrate hydrate adhesion/cohesion. Phys. *Chem. Chem. Phys*. **13**, 19796–19806. https://doi.org/10.1039/c1cp21907c

Aman, Z.M., Di Lorenzo, M., Kozielski, K., Koh, C.A., Warrier, P., Johns, M.L., May, E.F., 2016. Hydrate formation and deposition in a gas-dominant flowloop: Initial studies of the effect of velocity and subcooling. *J. Nat. Gas Sci. Eng*. **35**, 1490–1498. https://doi.org/10.1016/j.jngse.2016.05.015

Anklam, M. R., York, J. D., Helmerich, L., Firoozabadi, A., 2007. Effects of Antiagglomerants on the Interactions between Hydrate Particles. *AIChE J*. **54**, 565–574. https://doi.org/DOI 10.1002/aic.11378

Bethke, G.K., Snook, B., Herrera, G., Kelly, A.E., Joshi, S., Jain, S., 2018. A Novel Coating to Reduce Solids Deposition in Production Systems. *Offshore Technol. Conf*.

Brown, E., Hu, S., Wang, S., Wells, J., Koh, C., Nakatsuka, M., Veedu, V., 2017. Low-Adhesion coatings as a novel gas hydrate mitigation strategy. *Offshore Technol. Conf*.

Creek, J.L., Subramanian, S., Estanga, D., 2011. OTC 22017 New Method for Managing Hydrates in Deepwater Tiebacks. *Offshore Technol. Conf*. https://doi.org/10.4043/22017-MS

Ding, L., Shi, B., Wang, J., Liu, Y., Lv, X., Wu, H., Wang, W., Lou, X., Gong, J., 2017. Hydrate Deposition on Cold Pipe Walls in Water-in-Oil (W/O) Emulsion Systems. *Energy and Fuels* **31**, 8865–8876. https://doi.org/10.1021/acs.energyfuels.7b00559

Dirdal, E.G., 2013. Establishment of New Equipment for Testing Low Dosage Hydrate Inhibitors. University of Stavanger.

Ellison, B.T., Gallagher, C.T., Frostman, L.M., Lorimer, S.E., 2000. The Physical Chemistry of Wax, Hydrates, and Asphaltene. *Offshore Technol. Conf*. https://doi.org/10.4043/11963-MS

Gharbi, K., Benyounes, K., Khodja, M., 2017. Removal and prevention of asphaltene deposition during oil production: A literature review. *J. Pet. Sci. Eng*. **158**, 351–360. https://doi.org/10.1016/j.petrol.2017.08.062

Grasso, G.A., Sloan, E.D., Koh, C.A., Sum, A.K., Creek, J.L., Kusinski, G., 2014. OTC-25309 Hydrate Deposition Mechanisms on Pipe Walls. *Offshore T*. https://doi.org/10.4043/25309-MS

Kelland, M.A., 2014. Production Chemicals for the Oil and Gas Industry, 2nd Editio. ed. CRC Press.

Kinnari, K., Hundseid, J., Li, X., Askvik, K.M., 2015. Hydrate management in practice. *J. Chem. Eng. Data* **60**, 437–446. https://doi.org/10.1021/je500783u

Koh, C.A., Sloan, E.D., Sum, A.K., Wu, D.T., 2011. Fundamentals and Applications of Gas Hydrates. Annu. Rev. *Chem. Biomol. Eng*. **2**, 237–257. https://doi.org/10.1146/annurev-chembioeng-061010-114152

Kokal, S.L., Sayegh, S.G., 1995. Asphaltenes: The Cholesterol Of Petroleum. SPE 169–181. https://doi.org/10.2118/29787-MS

Lachance, J.W., Talley, L.D., Shatto, D.P., Turner, D.J., Eaton, M.W., 2012. Formation of hydrate slurries in a once-through operation. *Energy and Fuels* **26**, 4059–4066. https://doi.org/10.1021/ef3002197

Nicholas, Joseph W., Koh, Carolyn A., Sloan, E. Dendy, Nuebling, Lee, He, Helen, Horn, B., 2009. Measuring Hydrate/Ice Deposition in a Flow Loop from Dissolved Water in Live Liquid Condensate. *AIChE J*. **55**, 1882–1888. https://doi.org/https://doi.org/10.1002/aic.11874

Paso, K., Kompalla, T., Aske, N., Ronningsen, H.P., Oye, G., Sjoblom, J., 2009. Novel Surfaces with Applicability for Preventing Wax Deposition: A Review. *J. Dispers. Sci. Technol*. **30**, 757–781. https://doi.org/10.1080/01932690802643220

Patel, Zubin D., Russum, J., 2010. Flow Assurance: Chemical Inhibition of Gas Hydrates in Deepwater Production Systems. *Offshore Mag*.

Sloan, E. Dendy, Koh, Carolyn, Sum, Amadeu K., Ballard, Adam L., Creek, Jefferson, Eaton, Michael, Lachance, Jason, McMullen, Norm, Palermo, Thierry, Shoup, George, Talley, L., 2011. Natural Gas Hydrates in Flow Assurance, Natural Gas Hydrates in Flow Assurance. Gulf Professional Publishing. https://doi.org/10.1016/B978-1-85617-945-4.00009-1

Sloan, E.D., 2005. A changing hydrate paradigm - From apprehension to avoidance to risk management. *Fluid Phase Equilib*. **228–229**, 67–74. https://doi.org/10.1016/j.fluid.2004.08.009

Sloan, E.D., Koh, 2007. Clathrate Hydrates of Natural Gases, 3rd Edition. ed. CRC Press.

Smith, J.D., Meuler, A.J., Bralower, H.L., Venkatesan, R., Subramanian, S., Cohen, R.E., McKinley, G.H., Varanasi, K.K., 2012. Hydrate-phobic surfaces: Fundamental studies in clathrate hydrate adhesion reduction. *Phys. Chem. Chem. Phys*. **14**, 6013–6020. https://doi.org/10.1039/c2cp40581d

Sojoudi, H., Arabnejad, H., Raiyan, A., Shirazi, S.A., McKinley, G.H., Gleason, K.K., 2018. Scalable and durable polymeric icephobic and hydrate-phobic coatings. *Soft Matter* **14**, 3443–3454. https://doi.org/10.1039/c8sm00225h

Sojoudi, H., Walsh, M.R., Gleason, K.K., McKinley, G.H., 2015. Designing Durable Vapor-Deposited Surfaces for Reduced Hydrate Adhesion. *Adv. Mater. Interfaces* **2**, 1–12. https://doi.org/10.1002/admi.201500003

Sousa, A.L., Matos, H.A., Guerreiro, L.P., 2019. Preventing and removing wax deposition inside vertical wells: a review. *J. Pet. Explor. Prod. Technol*. https://doi.org/10.1007/s13202-019-0609-x

Speight, J.G., 2004. Petroleum asphaltenes - Part 1: Asphaltenes, resins and the structure of petroleum. *Oil Gas Sci. Technol*. **59**, 467–477. https://doi.org/10.2516/ogst:2004032

Srivastava, V., Majid, A.A.A., Warrier, P., Grasso, G., Chaudhari, P., Dendy Sloan, E., Koh, C.A., Wu, D.T., Zerpa, L.E., 2017. Hydrate Formation and Transportability Investigations in a High-Pressure Flowloop During Transient Shut-in / Restart Operations. *Offshore Technol. Conf*. 1–12. https://doi.org/10.4043/27849-MS

Tsai, L.C., Sheu, H.H., Chen, C.C., Ger, M. Der, 2015. The preparation of the chromized coatings on AISI 1045 carbon steel plate with the electroplating pretreatment of Ni or Ni/Cr-C film. *Int. J. Electrochem. Sci*. **10**, 317–331.

Turner, D., Boxall, J., Yang, D., Kleehamer, C., Koh, C., Miller, K., Sloan, E.D., 2005. Development of a Hydrate Kinetic Model and its Incorporation into the OLGA2000 Transient Multi-Phase Flow Simulator. *Proc. Fifth Int. Conf. Gas Hydrates*.

Urdahl, O., Lund, A., Mork, P., Nilsen, T.-N., 1995. Inhibition of Gas Hydrate Formation By Means of. *Chem. Eng. Sci*. **50**, 863–870. https://doi.org/10.1016/0009-2509(94)00471-3

Vargas, F. M., Tavakkoli, M., 2018. Asphaltene Deposition: Fundamentals, Prediction, Prevention, and Remediation, 1st Editio. ed. CRC Press.

Wang, S., Hu, S., Brown, E.P., Nakatsuka, M.A., Zhao, J., Yang, M., Song, Y., Koh, C.A., 2017. High pressure micromechanical force measurements of the effects of surface corrosion and salinity on CH4/C2H6hydrate particle-surface interactions. *Phys. Chem. Chem. Phys*. **19**, 13307–13315. https://doi.org/10.1039/c7cp01584d

Zhang, H., Yang, J., Chen, B., Liu, C., Zhang, M., Li, C., 2015. Fabrication of superhydrophobic textured steel surface for anti-corrosion and tribological properties. *Appl. Surf. Sci*. **359**, 905–910. https://doi.org/10.1016/j.apsusc.2015.10.191